

Collective Chaos

Tatsuo Shibata, Kunihiro Kaneko

*Department of Pure and Applied Sciences, University of Tokyo, Komaba, Meguro-ku, Tokyo 153,
Japan*

(February 5, 2008)

Abstract

An algorithm to characterize collective motion is presented, with the introduction of “collective Lyapunov exponent”, as the orbital instability at a macroscopic level. By applying the algorithm to a globally coupled map, existence of low-dimensional collective chaos is confirmed, where the scale of (high-dimensional) microscopic chaos is separated from the macroscopic motion, and the scale approaches zero in the thermodynamic limit.

05.45+b,05.90+m,64.60.Cn

Low-dimensional chaotic motion often arises from a system with many degrees of freedom. A classical example is chaos in a fluid system (such as Rayleigh-Bénard convection), where very high-dimensional chaotic motion should underlie at a molecular scale. A canonical answer for the condition to have low-dimensional chaos at a macroscopic level is given by separation of scales distinguishable from a microscopic level. Still it is not clear how such separation is possible, since chaos can lead to the amplification of a small-scale error.

To address the question, we note that a certain coupled dynamical system [1–6] shows some lower dimensional collective motion for macroscopic variables, while microscopic variables keep high dimensional chaos. To characterize such collective motion, Lyapunov exponent at a macroscopic scale will be introduced, which specifies the growth rate of error at macroscopic variables. By studying the dependence of the exponent on the length scale and the system size, it is shown how the “collective chaos” is compatible with microscopic chaos, and how they are separated at the ‘thermodynamic limit’.

Here we adopt a ‘heterogeneous’ globally coupled map (GCM) with a distributed parameter:

$$x_{n+1}(i) = (1 - \epsilon)f_i(x_n(i)) + \frac{\epsilon}{N} \sum_{j=1}^N f_j(x_n(j)) \quad (1)$$

where $x_n(i)$ is the variable of the i ’th element ($i = 1, 2, 3, \dots, N$) at discrete time n , and $f_i(x(i))$ is the internal dynamics for each element. For the dynamics we choose the logistic map $f_i(x) = 1 - a(i)x^2$, where the parameter $a(i)$ for the nonlinearity is distributed between $[a_0 - \frac{\Delta a}{2}, a_0 + \frac{\Delta a}{2}]$ as $a(i) = a_0 + \frac{\Delta a(2i-N)}{2N}$. As a macroscopic variable, we adopt the mean field,

$$h_n = \frac{1}{N} \sum_{i=1}^N f_i(x_n(i)). \quad (2)$$

in which the collective motion is contained. On the other hand, chaos of $x_n(i)$ is referred to ‘microscopic’ here.

Conventional GCM with identical parameters is given by $\Delta a = 0$, whose study has revealed clustering, chaotic itinerancy, partial ordering, and so forth [7]. In particular,

study of collective dynamics has gathered much attention [1–4]. When the coupling ϵ is small enough, oscillation of each element is mutually desynchronized, and the effective degrees of freedom increase in proportion to the number of elements N . Still, a macroscopic variable is found to show some kind of ordered motion distinguishable from noise, ranging from torus to high-dimensional chaos [1–4].

For instance, Fig.1 gives a return map of the mean field dynamics of our model (1), which shows some pattern that may suggest low-dimensional chaos. Torus motion is also found by changing the parameters [4]. Here we try to characterize such collective dynamics, and search for low-dimensional collective chaos.

First note that the conventional Lyapunov exponents are not relevant to the characterization of collective motion. Indeed, for small ϵ , all the N Lyapunov exponents of (1) are positive (whose values are close to the exponent of a single logistic map $x \rightarrow f_i(x)$). No exponent corresponding to the mean field motion is observed in this spectrum of N exponents. This apparent paradox can be resolved by noting the order of limit to define the Lyapunov exponent. In the calculation of the Lyapunov spectrum we take a 0 limit of disturbance applied to the orbit. As long as we choose this limit first and then the thermodynamic limit ($N \rightarrow \infty$), the N Lyapunov exponents cannot characterize the collective motion [8]. It is necessary to take the thermodynamic limit first and then the limit of disturbance scale, to characterize the collective dynamics.

Since we are concerned with a system of large but finite N , the above order of limit implies that we have to keep the disturbance amplitude finite. To study such orbital instability, the finite-size Lyapunov exponent introduced by Vulpiani and his coworkers [9] is useful. It is given by

$$\lambda_{\delta_0}(\Delta) = \left\langle \frac{1}{\tau} \log \frac{\Delta}{\delta_0} \right\rangle, \quad (3)$$

where τ is the maximum time such that $|x'_n - x_n| < \Delta$ for trajectories x_n and x'_n starting from x_0 and $x'_0 = x_0 + \delta_0$ respectively, while $\langle \cdot \rangle$ is an average over the trajectories starting from different initial values. The length scale Δ can be considered as the scale of observation.

We have measured the finite-size Lyapunov exponent for the macroscopic variable h_n of our GCM (1). Here we perturb the orbit to give rise to a change from h_0 to $h'_0 = h_0 + \delta_0$ (see the caption of Fig.2 for detailed description). In Fig.2, the finite-size Lyapunov exponent is plotted with the change of Δ .

As long as the system size is finite, this finite-size Lyapunov exponent reflects not only the macroscopic motion but also the microscopic chaos. Indeed the exponent in Fig.2 changes with the scale Δ and no clear plateau (except for $\delta_0 \rightarrow 0$) is visible. On the other hand, if low-dimensional macroscopic dynamics has a characteristic time scale separated from the microscopic dynamics, it will be possible to extract the growth rate of perturbation in the collective motion from the finite-size Lyapunov exponent for the macroscopic variable. To do so, we postulate the following assumptions that are expected to hold if the collective dynamics is low-dimensional chaos or on a torus.

First note that in the limit, $\Delta \rightarrow 0$ and $\delta_0 \rightarrow 0$, the finite-size Lyapunov exponent $\lambda_{\delta_0}(\Delta)$ converges to maximum Lyapunov exponent λ_m , which is determined by the conventional Lyapunov exponents for the microscopic variables $x_n(i)$ directly.

Considering that the collective dynamics appears by coarse-grained macroscopic variables, we postulate that there are length scales (in the phase space) $\Delta \in [\Delta_m, \Delta_C]$, where the macroscopic variable is characterized by “collective Lyapunov exponent” λ_C . Below $\Delta < \Delta_m$ the microscopic chaos dominates, while the orbit is out of the attractor (at a macroscopic level) for $\Delta > \Delta_C$. To have low-dimensional collective dynamics, it is postulated that λ_C is independent of N (as long as it is large enough), and that Δ_m should approach zero with $N \rightarrow \infty$ while Δ_C remains finite.

Based on the above assumptions, we can derive an approximate form of the finite-size Lyapunov exponent against the scale Δ . Let δ_n denote the distance from the original trajectory at time step n . For the scale $\Delta < \Delta_m$, δ_n increases proportionally with $\exp(\lambda_m n)$. Hence $\tau(\Delta) = \frac{1}{\lambda_m} \log \frac{\Delta}{\delta_0}$ follows, independently of the collective dynamics.

On the other hand, for the scale $\Delta_m < \Delta < \Delta_C$, δ_n is given as $\delta_n \propto \exp(\lambda_C n)$ for a chaotic case with $\lambda_C > 0$, or $\delta_n \propto n^\kappa$ for a torus case with κ as a certain constant. Corresponding

to each collective motion, $\tau(\Delta)$ and the finite-size Lyapunov exponent $\lambda_{\delta_0}(\Delta)$ are given by

$$\tau(\Delta) = \begin{cases} \frac{1}{\lambda_C} \log \frac{\Delta}{\Delta_m} + \frac{1}{\lambda_m} \log \frac{\Delta_m}{\delta_0} & (\text{chaotic case}) \\ \left(\frac{\Delta}{\Delta_m}\right)^{\frac{1}{\kappa}} + \frac{1}{\lambda_m} \log \frac{\Delta_m}{\delta_0} - 1 & (\text{torus case}) \end{cases}, \quad (4)$$

and

$$\lambda_{\delta_0}(\Delta) = \begin{cases} \frac{\lambda_m \lambda_C \log \frac{\Delta}{\delta_0}}{\lambda_C \log \frac{\Delta_m}{\delta_0} + \lambda_m \log \frac{\Delta}{\Delta_m}} & (\text{chaotic case}) \\ \frac{\log \frac{\Delta}{\delta_0}}{\frac{1}{\lambda_m} \log \frac{\Delta_m}{\delta_0} + \left(\frac{\Delta}{\Delta_m}\right)^{\frac{1}{\kappa}} - 1} & (\text{torus case}) \end{cases}. \quad (5)$$

Fig.3 shows the behavior of $\lambda_{\delta_0}(\Delta)$ for our GCM, with a fitting curve by Eq.(5). Here the parameters λ_C and Δ_m are obtained to fit the data for several values of δ_0 and Δ . The estimated exponent λ_C is positive, and is much smaller than the Lyapunov exponent λ_m for microscopic chaos. Thus there is a regime in which the mean field dynamics shows low dimensional chaotic dynamics, although there is no clear plateau corresponding to λ_C . The value λ_C is smaller than $\lambda_{\delta_0}(\Delta)$.

It is then necessary to study N dependence of Δ_m , in order to confirm the existence of the low-dimensional collective motion. For this, it is convenient to transform Eq.(5) to remove δ_0 dependence of the data. For it, we define $t(\Delta)$ as $t(\Delta) = \tau(\Delta) + \frac{1}{\lambda_m} \log \delta_0$, which characterizes the time for amplification of error from a certain scale independent of δ_0 . From Eq.(4), we obtain

$$t(\Delta) = \begin{cases} \frac{1}{\lambda_C} \log \Delta + \left(\frac{1}{\lambda_m} - \frac{1}{\lambda_C}\right) \log \Delta_m & (\text{chaotic case}) \\ \left(\frac{\Delta}{\Delta_m}\right)^{\frac{1}{\kappa}} + \frac{1}{\lambda_m} \log \Delta_m - 1 & (\text{torus case}) \end{cases}. \quad (6)$$

Thus, the N dependence of Δ_m appears as a shift of constant in $t - \Delta$ plot, while λ_C or κ is given by a slope in a suitable plot.

In Fig.4, t is plotted as a function of Δ . As is shown in Fig.4(a), the slope of the semi-log plot is independent of N . The Lyapunov exponent λ_C , characterizing the collective motion, is given by the inverse of the slope, and is estimated as 0.02. On the other hand, Δ_m , given by the shift of the plots, decreases with N , while Δ_C does not show significant change. Thus the scale for the collective motion $\Delta_m < \Delta < \Delta_C$ increases with N . In Fig.5, N dependence

of Δ_m is plotted, which gives $\Delta_m \sim \frac{1}{\sqrt{N}}$, whose form is expected from the central limit theorem. Hence the emergence of low-dimensional collective chaos at the thermodynamic limit is confirmed.

We have also applied the present algorithm to the case with a collective torus motion. Fig.4(b), $(t - \Delta)$ plot, shows that κ , the inverse of the slope, is 0.5, independent of N . Indeed this exponent $1/2$ is expected from the diffusion process of phase on the torus. The decrease of Δ_m with N is also plotted in Fig.5, which again shows the expected decrease of $\Delta_m \sim \frac{1}{\sqrt{N}}$. Hence the collective torus motion is demonstrated.

In this letter, we have proposed an algorithm to characterize the collective (chaotic) motion, and applied it to a GCM. We have introduced collective Lyapunov exponent, to characterize the growth rate of perturbation in the collective motion. The microscopic chaotic motion exists at a small scale of the macroscopic variable, but such scale Δ_m is shown to decrease as $1/\sqrt{N}$. Hence, the macroscopic motion is separated from the microscopic motion and the emergence of low-dimensional collective motion with $N \rightarrow \infty$ is confirmed.

Existence of low-dimensional collective chaos in the presence of microscopic chaos has often been suspected [10]. Indeed for a GCM with homogeneous elements (i.e., with $\Delta a = 0$), such low-dimensional collective chaos has not been observed so far. In Fig.4(c), we have also applied our algorithm to this case. The separation of scales is not clear and the data cannot be fitted with (6). The shift of the plot gets smaller with the increase of N . At least Δ_m does not decrease as $1/\sqrt{N}$ [11].

Our $t - \Delta$ plot provides a tool to distinguish low-dimensional collective chaos from high-dimensional one. In the former case, the plot shifts as $\log(\sqrt{1/N})$ with N , while for the latter case such shift is not observed. This distinction generally holds, even if the approximation to get (6) may not be very good [13].

Our estimation of macroscopic motion is realized for a system subjected to microscopic chaos. It is expected that our algorithm can be applied even if we do not know the equation of motion, since the method of [9] is based on Wolf's algorithm [12] developed for the estimate of Lyapunov exponents from experimental data. Thus, we hope that our method developed

in this letter is applicable to data obtained from experiments.

The authors thank the Supercomputer Center, Institute for Solid State Physics, University of Tokyo for the facilities. This work is partially supported by a Grant-in-Aid for Scientific Research from the Ministry of Education, Science, and Culture of Japan.

REFERENCES

- [1] K. Kaneko, Phys. Rev. Lett. **65**, 1391 (1990); Physica **D55**, 368 (1992). G. Perez and H. A. Cerdeira, Phys. Rev. **A46**, 7492 (1992); Physica **D63**, 341 (1993). S. V. Ershov, A. B. Potapov, Physica **D86**, 532 (1995); Physica **D106**, 9 (1997). S. Morita, Phys. Lett. **A211**, 258 (1996). T. Chawanya, S. Morita, Physica, **D116**, 44 (1998). N. Nakagawa, T. Komatsu, Phys. Rev. **E57**, 1570 (1998).
- [2] A. S. Pikovsky, J. Kurths, Phys. Rev. Lett. **72**, 1644 (1994); Physica **D76**, 411 (1994).
- [3] K. Kaneko, Physica **D86**, (1995) 158.
- [4] T. Shibata, K. Kaneko, Europhysics Letters **38(6)**, 417 (1997); preprint (1998) (xxx.lanl.gov chao-dyn/9802018, submitted to Physica **D**).
- [5] H. Chaté, P. Manneville, Prog. Theor. Phys. **87**, 1 (1992).
- [6] N. Nakagawa, K. Kuramoto, Physica **D80**, 307 (1995). M.-L. Chabanol, V. Hakim, W.-J. Rappel, Physica **D103**, 273 (1997).
- [7] K. Kaneko, Physica **D41**, 137 (1990).
- [8] For example, all of the N Lyapunov exponents are positive, even if there appears quasiperiodic motion for the collective variable h_n as N goes to infinity [4].
- [9] G. Paladin, M. Serva, A. Vulpiani, Phys. Rev. Lett. **74**, 66 (1995); E. Aurell, et al., Phys. Rev. Lett. **77**, 1262 (1996).
- [10] T. Bohr, G. Grinstein, Y. He, C. Jayaprakash, Phys. Rev. Lett. **85**, 2155 (1987).
- [11] Hence, the scale of the macroscopic motion in GCM with $\Delta a = 0$, is not separated from the microscopic dynamics. This gives a crucial difference between the ‘heterogeneous’ GCM and ‘identical’ GCM.
- [12] A. Wolf, J. B. Swift, H. L. Swinney, J. A Vastano, Physica **D16**, 285 (1985).

[13] After the completion of the present manuscript, the authors are informed of the recent preprint by M. Cencini, M. Falcioni, D. Vergni, A. Vulpiani ([xxx.lanl.gov chaos-dyn/9804045](http://xxx.lanl.gov/chaos-dyn/9804045)), where a related study to the collective chaos is presented.

FIGURES

FIG. 1. An example of return map for chaotic collective motion. $a_0 = 1.92$, $\Delta a = 0.088$, $\epsilon = 0.1$, $N = 10^7$. Points (h_n, h_{n+1}) are plotted over 3×10^4 steps after transient are discarded.

FIG. 2. $\lambda_{\delta_0}(\Delta)$ is plotted for the model (1) with $a_0 = 1.92$, $\Delta a = 0.088$, $\epsilon = 0.1(\odot)$, $a_0 = 1.9$, $\Delta a = 0.05$, $\epsilon = 0.098(\times)$, $a_0 = 1.9$, $\Delta a = 0.05$, $\epsilon = 0.11(\triangle)$, $a_0 = 1.69755$, $\Delta a = 0.0$, $\epsilon = 0.008(\square)$, with $N = 10^7$. Initial perturbation amplitude δ_0 is fixed at 1.0×10^{-7} . For computation, displacement $h'_0 = h_0 + \delta_0$ is created by perturbing the orbit as $x'_0(i) = x_0(i) + \delta_0 \times \sigma$, where σ is a random number in $[-1, 1]$. Each point is obtained by averaging over 100 samples. Specific choice of this perturbation scheme is irrelevant to our results, as long as the collective variable is perturbed. Adopting the algorithm to be presented, the collective motion is shown to be torus (\triangle), low-dimensional chaos (\odot and \times), and high-dimensional chaos (\square).

FIG. 3. The finite-size Lyapunov exponent $\lambda_{\delta_0}(\Delta)$ is plotted as a function of Δ for several initial displacement δ_0 . The exponent is computed from the average over 100 samples starting from different initial condition. The curve from Eq.(5) fitted to the data is also indicated. From the fitting, $\Delta_m = 0.00086$ and $\lambda_C = 0.02$ are obtained, while $\lambda_m = 0.41$ is directly obtained from Eq.(1). $a_0 = 1.9$, $\Delta a = 0.05$, $\epsilon = 0.098$, and $N = 10^6$. Note that although $\lambda_{\delta_0}(\Delta)$ for small Δ is slightly smaller than λ_m , it approaches λ_m with $\delta_0 \rightarrow 0$.

FIG. 4. The normalized time steps $t(\Delta)$ are plotted for $N = 10^4$, 10^5 , 10^6 , and 10^7 , with the fitted curves(6). (a) *chaotic case* (with a semi-log plot), for $a_0 = 1.9$, $\Delta a = 0.05$, $\epsilon = 0.098$. (b) *torus case* (with a log-log plot), for $a_0 = 1.9$, $\Delta a = 0.05$, $\epsilon = 0.11$. The maximum Lyapunov exponent $\lambda_m = 0.41$ (a), 0.39 (b) are obtained directly from our model(1). The parameters obtained by a least square fitting algorithm give $\lambda_C = 0.02$.(a), $\kappa = 0.5$ (b). (c) *high-dimensional case*, which does not obey Eq.(6), (with a semi-log plot), for $a_0 = 1.6962$, $\Delta a = 0$, $\epsilon = 0.008$. In this case, while the return map shows some structure, t for $N = 10^6$ and 10^7 are not separated any more.

FIG. 5. The microscopic length scales Δ_m are plotted as a function of N for several parameters. Δ_m is obtained from the fitting indicated in Fig.4. The parameters are $a_0 = 1.92$, $\Delta a = 0.088$, $\epsilon = 0.1(\odot, \text{chaos})$, $a_0 = 1.9$, $\Delta a = 0.05$, $\epsilon = 0.098(\times, \text{chaos})$, $a_0 = 1.9$, $\Delta a = 0.05$, $\epsilon = 0.11(\triangle, \text{torus})$,

Fig. 1 T. Shibata & K. Kaneko

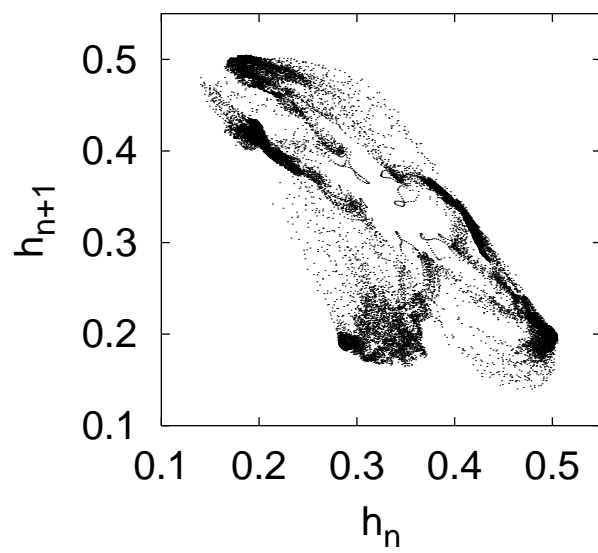


Fig. 2 T. Shibata & K. Kaneko

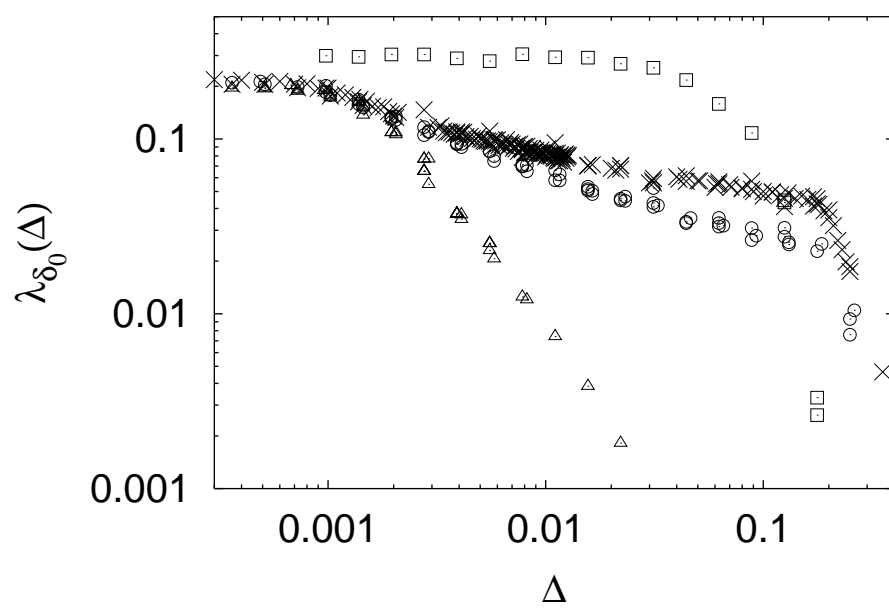


Fig.3 T. Shibata & K. Kaneko

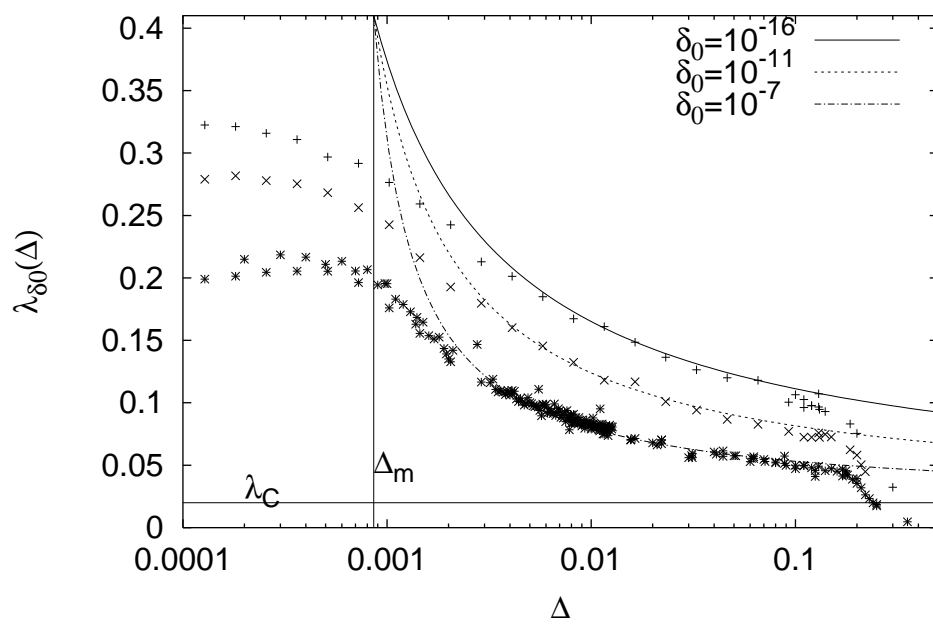


Fig.4(a) T. Shibata & K. Kaneko

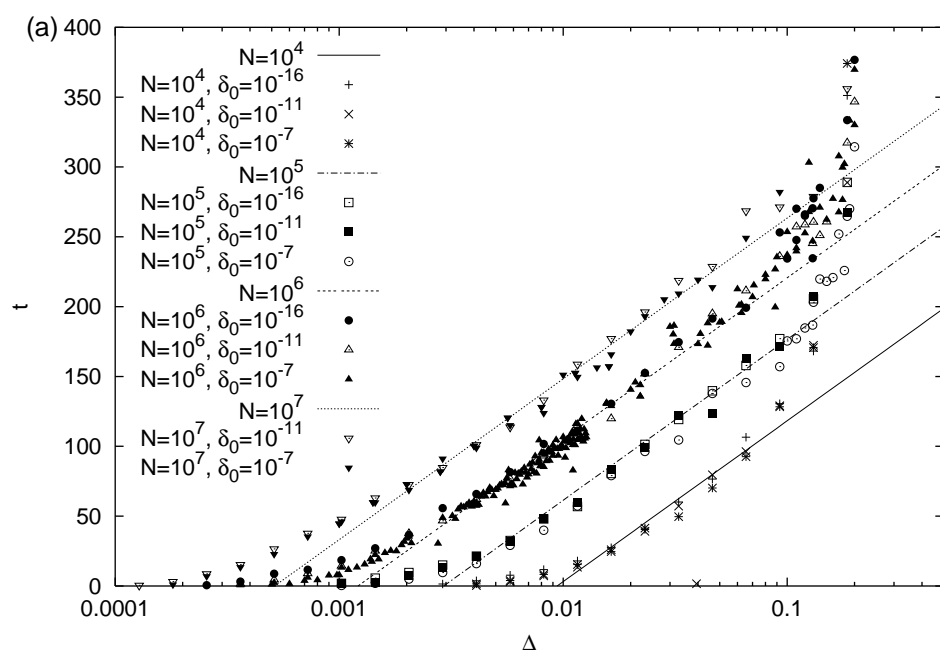


Fig.4(b) T. Shibata & K. Kaneko

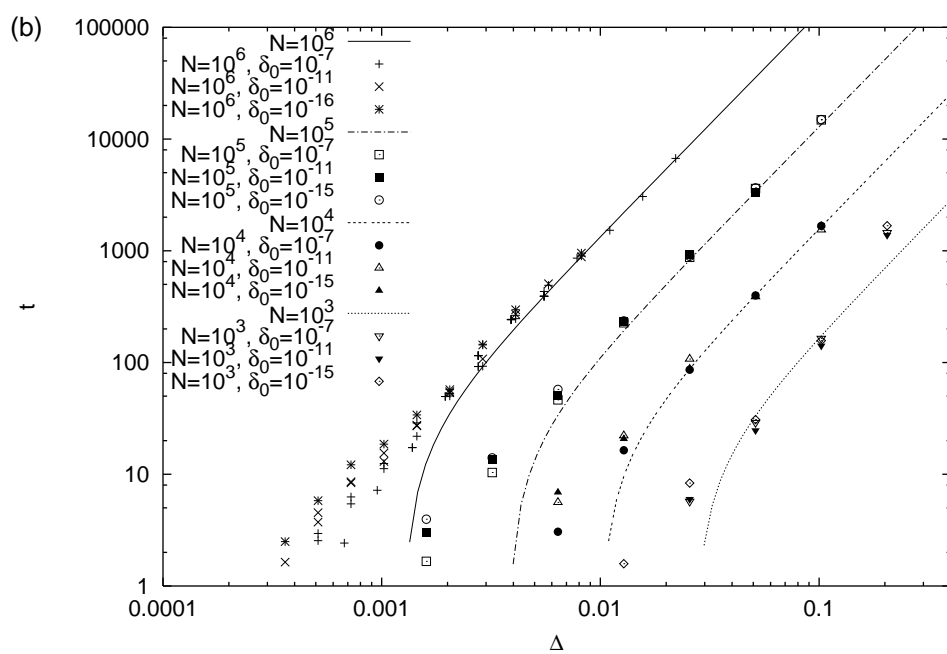


Fig.4(c) T. Shibata & K. Kaneko

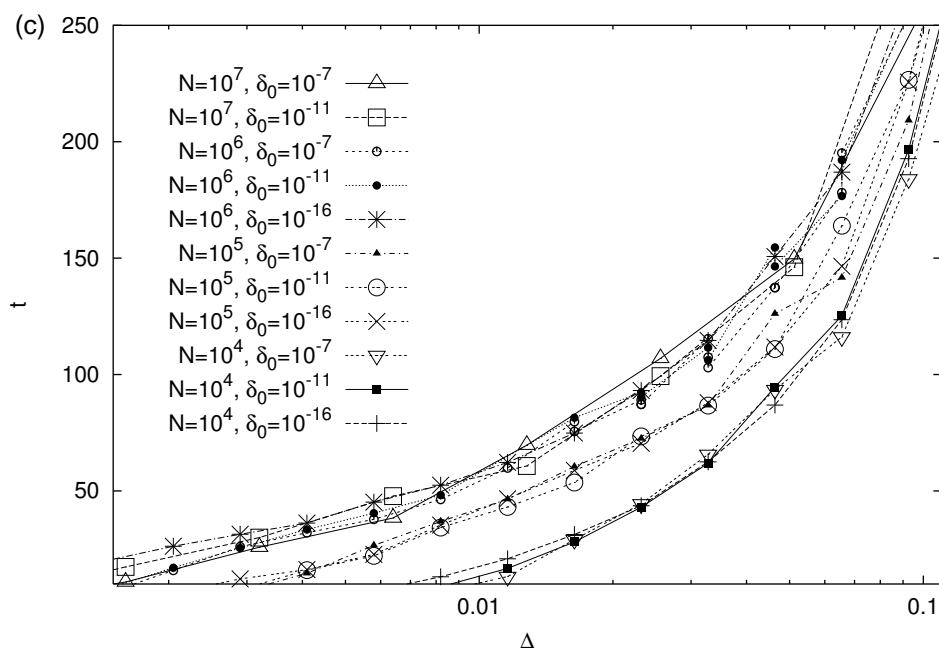


Fig.5 T. Shibata & K. Kaneko

